Theor Chem Acc (2003) 110: 218–223
DOI 10.1007/s00214-003-0467-x

Theoretical
Chemistry Accounts

Regular article

The electronic spectrum of VCr

K. Andersson

Department of Theoretical Chemistry, Chemical Centre, University of Lund, P.O. Box 124, 221 00 Lund, Sweden

Received: 22 March 2002 / Accepted: 20 November 2002 /

Abstract. The electronic spectrum of VCr has been studied using the complete-active-space self-consistent field complete-active-space second-order perturbation theory approach. Potential-energy curves for 12 electronic states have been computed. Transition energies, with respect to the $X^2\Delta$ ground state, for some of the calculated electronic states are (with possible experimental values within parentheses) 0.53 eV (0.56) for $A^2\Sigma^+$, 1.03 eV (1.14) for $A^4\Delta$, 1.20 eV (1.14) for $B^2\Delta$, 1.45 eV (1.51) for $B^4\Delta$, 1.60 eV (1.51, 1.78) for $C^2\Delta$, and 1.61 eV (1.63) for $A^4\Sigma^-$.

Keywords: Complete-active-space self-consistent field/complete-active-space second-order perturbation theory – Potential-energy curves – Spectroscopic constants

1 Introduction

Some years ago the electronic spectrum of Cr_2 was studied using the complete-active-space self-consistent field (CAS–SCF)/CAS second-order perturbation theory (PT2) approach [1, 2]. Altogether 18 states were calculated. Despite the complicated electronic structure involving multiple metal-metal bonding the chromium dimer was successfully described using this approach. Through the calculations it was possible to give explanations for or to verify some of the experimental results that had appeared in the literature, for example, the shape of the ground-state potential-energy curve.

When working on the electronic spectrum of Cr_2 the experimental work by Casey and Leopold (using negative ion photoelectron spectroscopy) [3] constituted a great source of inspiration and information. Later on Alex and Leopold did experiments on the VCr molecule using similar techniques. The results of this work constituted a part of the thesis of Alex [4] and they have also been published elsewhere [5]. Encouraged by the successful calculations on Cr_2 and inspired by the experimental results on VCr it was decided to also perform calculations on VCr using the CASSCF/CASPT2 approach.

One difference between Cr_2 and VCr, which will be of importance in the calculations, is demonstrated in Tables 1 and 2. Here the lowest atomic energy levels of the chromium and vanadium atoms are collected. For the vanadium atom the energy difference between the two lowest states is only 0.245 eV. More important is that they differ in the electronic configuration. The ^4F ground state has two 4*s* electrons, while the ^6D first excited state has only one 4*s* electron. The differing electronic configuration is important in CASSCF calculations using a small active space (3d and 4s). By using orbitals optimized for one state the energy for the other state will increase by about 2 eV from its optimized value.[1]

The discussion in the previous paragraph is of importance when forming the molecular orbitals for VCr. From the experimental atomic excitation energies in Tables 1 and 2 the excitation energies for the lowest-lying states of VCr at infinite separation can be calculated. These data are assembled in Table 3 together with the molecular states. From a simple molecular orbital picture the $3d\delta$ orbitals form the least-bonding orbitals, resulting in a $^2\Delta$ ground state for VCr. From Table 3 some interesting observations can be made. First, the $^2\Delta$ ground state correlates with the (^6D,^7S) separated-atom limit (therefore the energy of the ^6D atomic state of vanadium was set to zero in Table 2). Thus, upon dissociation the ground state of VCr will not separate into the ground state of the vanadium atom. Second, from the previous discussion it is clear that it is not possible to describe the molecular states correlating with the (^4F,^7S) and the (^6D,^7S) separated-atom limits using the same set of orbitals. This might be problematic since some of the molecular states are mixtures of (^4F,^7S) and (^6D,^7S). The $^4\Delta$ states give a good illustration. The state lowest in energy is dominated by (^4F,^7S) at long internuclear

Contribution to Björn Roos Honorary Issue

e-mail: kerstin.andersson@kau.se

---

[1] 1.82 eV for ^4F and 2.26 eV for ^6D

Table 1. The lowest atomic energy levels of Cr

Configuration	Designation	Energy (eV)[a]
$3d^54s$	^{5}G	2.544
$3d^44s^2$	^{5}D	1.003
$3d^54s$	^{5}S	0.941
$3d^54s$	^{7}S	0.000

[a] Averaged over J and M_J components. The energy values (experimental) taken from Ref. [15]

Table 2. The lowest atomic energy levels of V

Configuration	Designation	Energy (eV)[a]
$3d^34s^2$	^{2}D	1.517
$3d^34s^2$	^{2}P	1.427
$3d^34s^2$	^{2}G	1.080
$3d^34s^2$	^{4}P	0.920
$3d^44s$	^{4}D	0.781
$3d^44s$	^{6}D	0.000
$3d^34s^2$	^{4}F	−0.245

[a] Averaged over J and M_J components. The energy values (experimental) taken from Ref. [15]

distances and (^{6}D,^{7}S) at short internuclear distances, which can be explained by the fact that the state correlating with (^{4}F,^{7}S) has one more electron in the 4s atomic orbital (which is more diffuse than 3d). When the molecule is formed there will be less screening of the nuclei and the potential curve should become more repulsive at longer distances than the potential curve for the state correlating with (^{6}D,^{7}S). To describe the $^4\Delta$ states properly with a small active space is difficult especially at intermediate distances where the molecular orbitals are changing considerably. The two $^4\Delta$ states correlating with (^{4}F,^{7}S) and (^{6}D,^{7}S) thus can be considered as two local minima with a high barrier in between on the CASSCF surface (as a function of configuration interaction coefficients and molecular orbitals).

From the previous discussion one can conclude that the calculation of the lowest-lying electronic states of VCr might be more problematic than that for Cr_2, at least at intermediate bond distances. However, at equilibrium bond distances it should be possible to perform accurate calculations and to obtain accurate spectroscopic data for a number of electronic states.

2 Methodology

The computational model used for calculating the electronic spectrum of VCr is similar to the one used for Cr_2 [2]. CASSCF wave functions were formed by distributing 11 electrons in the 3d and 4s derived active orbitals (keeping the inactive $1s, 2s, 2p, 3s$, and $3p$ derived orbitals doubly occupied) either in single-state calculations or in state-average calculations (see later). The remaining dynamical electron correlation energy was obtained through second-order perturbation theory (CASPT2) [6, 7]. To the Fock matrix, defining the zeroth-order Hamiltonian, a correction (denoted $\mathbf{g}_1$ in Ref. [8]) was added for an enlargement of the energy gap between active and secondary orbitals. Further, the correlation of $1s, 2s$, and $2p$ electrons was ignored and relativistic corrections were added at the CASSCF level of theory using first-order perturbation theory. The main differences between the calculation on Cr_2 [2] and the present calculation on VCr are

1. g-type functions were included for VCr.
2. The 3s and 3p electrons were not correlated for VCr.
3. Intruder states in the CASPT2 calculation on VCr were removed by introducing a level shift operator (0.30 H) in the zeroth-order Hamiltonian [9].

Although the computational model used for Cr_2 gives results in agreement with many experimental data (one exception is the bond length of the ground state, which is in error by 0.035 Å) it was shown in a later study on the ground state and the second excited $^3\Sigma_u^+$ state that the results suffer from a large basis set superposition error (BSSE) [9]. This affects mainly the binding energy, which is decreased by about 0.3 eV when the BSSE is taken into account (see the basis A results in Table 4). In the same study the effect of including two g-type basis functions on properties of Cr_2 was demonstrated (see the basis B results in Table 4). With g-type functions included a better agreement with experiment of the bond length and binding energy of the ground state is obtained and these are now in error by 0.007 Å and about 0.1 eV, respectively. The transition energy to the second excited $^3\Sigma_u^+$ state is also improved; however, the vibrational frequencies deteriorate and deviate from experimental values by about 100 cm^{-1} owing to too large an increase in energy in the region between the

Table 3. Separated-atom limits and molecular states for VCr

Separated-atom limit	Energy (eV)[a]	Molecular states[b]
^{2}D, ^{7}S	1.517	$^{6,8}\Sigma^+$, $^{6,8}\Pi$, $^{6,8}\Delta$
^{2}P, ^{7}S	1.427	$^{6,8}\Sigma^-$, $^{6,8}\Pi$
^{2}G, ^{7}S	1.080	$^{6,8}\Sigma^+$, $^{6,8}\Pi$, $^{6,8}\Delta$, $^{6,8}\Phi$, $^{6,8}\Gamma$
^{6}D, ^{5}D	1.003	$^{2,4,6,8,10}\Sigma^+(3)$, $^{2,4,6,8,10}\Sigma^-(2)$, $^{2,4,6,8,10}\Pi(4)$, $^{2,4,6,8,10}\Delta(3)$, $^{2,4,6,8,10}\Phi(2)$, $^{2,4,6,8,10}\Gamma$
^{6}D, ^{5}S	0.941	$^{2,4,6,8,10}\Sigma^+$, $^{2,4,6,8,10}\Pi$, $^{2,4,6,8,10}\Delta$
^{4}P, ^{7}S	0.920	$^{4,6,8,10}\Sigma^-$, $^{4,6,8,10}\Pi$
^{4}D, ^{7}S	0.781	$^{4,6,8,10}\Sigma^+$, $^{4,6,8,10}\Pi$, $^{4,6,8,10}\Delta$
^{4}F, ^{5}D	0.758	$^{2,4,6,8}\Sigma^+(2)$, $^{2,4,6,8}\Sigma^-(3)$, $^{2,4,6,8}\Pi(5)$, $^{2,4,6,8}\Delta(4)$, $^{2,4,6,8}\Phi(3)$, $^{2,4,6,8}\Gamma(2)$, $^{2,4,6,8}H$
^{4}F, ^{5}S	0.696	$^{2,4,6,8}\Sigma^-$, $^{2,4,6,8}\Pi$, $^{2,4,6,8}\Delta$, $^{2,4,6,8}\Phi$
^{6}D, ^{7}S	0.000	$^{2,4,6,8,10,12}\Sigma^+$, $^{2,4,6,8,10,12}\Pi$, $^{2,4,6,8,10,12}\Delta$
^{4}F, ^{7}S	−0.245	$^{4,6,8,10}\Sigma^-$, $^{4,6,8,10}\Pi$, $^{4,6,8,10}\Delta$, $^{4,6,8,10}\Phi$

[a] The energy values taken from Tables 1 and 2

[b] Molecular states derived using the Wigner–Witmer rules, as described in Ref. [16]

Table 4. Properties of two states of Cr_2. The effects of including the basis set superposition error (BSSE), g-type functions, and 3*s* and 3*p* electron correlation are demonstrated

Method[a]	Shift[b] (H)	Basis[c]	r_e (Å)	$\Delta G_{1/2}$ (cm^{-1})	D_0 (eV)	T_e (eV)
The $X^1\Sigma_g^+$ ground state:						
CASPT2 + RC + 3*s*3*p*[d]	0.20	A	1.714	467	1.422	0
CASPT2 + RC + 3*s*3*p* + BSSE[d]	0.20	A	1.724	450	1.144	0
CASPT2 + RC + 3*s*3*p* + BSSE[d]	0.20	B	1.686	535	1.538	0
CASPT2 + RC	0.30	C	1.669	589	1.577	0
Exp.	–	–	1.679[e]	452[e]	1.443 ± 0.056[f]	0
The second $^3\Sigma_u^+$ excited state:						
CASPT2 + RC + 3*s*3*p*[d]	0.20	A	1.656	591	0.923	1.80
CASPT2 + RC + 3*s*3*p* + BSSE[d]	0.20	A	1.663	564	0.602	1.84
CASPT2 + RC + 3*s*3*p* + BSSE[d]	0.20	B	1.643	667	1.003	1.79
CASPT2 + RC	0.30	C	1.659	687	0.822	1.85
Exp.	–	–	1.65 ± 0.02[g]	574[g]	–	1.76[g]

[a] + RC: relativistic corrections are included (see text); + 3*s*3*p*: 3*s* and 3*p* electron correlation effects are included, + BSSE: basis set superposition error is included

[b] The size of the level-shift operator for removing intruder states [9]

[c] A: atomic natural orbital (8s7p6d4f) [1]; B: atomic natural orbital (8s7p6d4f2g) [9]; C: atomic natural orbital (6s5p4d3f2g) [10]

[d] Ref. [9]

[e] Ref. [17]

[f] Ref. [18]

[g] Ref. [3]

3*d*–3*d* and 4*s*–4*s* binding [9]. Except for the vibrational frequencies the inclusion of g-type basis functions improves the spectroscopic properties of Cr_2 and they seem to be important for obtaining accurate bond lengths.

The disadvantage of the computational model described earlier and in Ref. [9] is that the BSSE has to be calculated, which leads to quite cumbersome calculations. However, as was shown in Ref. [9] a major part of the BSSE stems from correlating the 3*s* and 3*p* electrons. By excluding the 3*s* and 3*p* electron correlation the BSSE is rather small (around 0.05 eV at equilibrium) and there is no need to calculate it. Therefore an atomic natural orbital basis set of the size 6s5p4d3f2g from Ref. [10] was selected and calculations of the ground state and the second excited $^3\Sigma_u^+$ state of Cr_2 were repeated without the inclusion of 3*s* and 3*p* electron correlation. The results are shown in Table 4 (see the basis C results) and they are in comparable agreement with the previously discussed basis B results which included 3*s* and 3*p* electron correlation. The errors compared with experimental data are 0.01 Å in bond lengths, 150 cm^{-1} in vibrational frequencies, and 0.1 eV in transition energies. This last procedure seems to be a good compromise between accuracy and computational cost and it is the one which is going to be adopted for the calculation of the electronic spectrum of VCr. As was demonstrated in the Cr_2 calculations good accuracy can be expected for bond lengths and transition energies. For vibrational frequencies, the errors can be as large as 150 cm^{-1}.

About 30 points on each potential curve were computed with a spacing of 0.05 au around the minimum. The vibrational Schrödinger equation was solved by numerical integration and spectroscopic constants were computed by a least-squares fit to the calculated vibrational energy levels. Since the intruder states have been removed the accuracy for calculating spectroscopic constants should be good using this procedure. For some states there are two minima on the potential curve and for those cases the calculated spectroscopic properties refer to the inner minimum.

The calculations were performed using the MOLCAS version 4.0 quantum chemistry software [11].[2] However, due to curve crossings a multistate version of CASPT2 [12], not included in MOLCAS version 4.0, was used for two electronic states.

3 Details of the calculation

Following the discussion in the introduction VCr ought to have a $^2\Delta$ ground state. From Table 3 it is clear that the separated-atom limit for the lowest $^2\Delta$ state is (^{6}D,^{7}S). One Δ component spans the same irreducible representation as Σ^+ in C_{2v} and an energy-average CASSCF calculation, using the same set of orbitals, for $X^2\Delta$ and $A^2\Sigma^+$ was performed followed by CASPT2 calculations for each of the two states.

The same procedure as previously was initially used for the corresponding quartet states ($A^4\Delta$ and $A^4\Sigma^+$); however, since there are altogether three $^4\Delta$ states and three $^4\Sigma^+$ states in Table 3 with one electron in 4*s* for each of the two atoms in the separated atom limit [(^{6}D,^{7}S), (^{4}D,^{7}S), and (^{6}D,^{5}S)] an energy-average CASSCF calculation for $A^4\Delta$, $B^4\Delta$, $C^4\Delta$, $A^4\Sigma^+$, $B^4\Sigma^+$, and $C^4\Sigma^+$ was performed followed by CASPT2 calculations for each of the six states. By starting at infinite distance (using orbitals from the doublet calculation, for instance) it was straightforward to generate the entire

---

[2] Owing to problems in calculating natural orbitals in the CASSCF program (part of the restricted-active-space (RAS) SCF program) this part of the code was omitted. This is possible since the whole inactive space is frozen in the CASPT2 calculations, giving a well-defined second-order energy no matter which orbitals are used as long as the CASSCF energy is converged

potential curves (from long to short bond distances) even though the six states were not lowest in energy at all distances. The CASPT2 potential curves for the $A^4\Delta$ and $A^4\Sigma^+$ states from this six-state energy-average calculation are almost parallel to the corresponding curves obtained in the two-state energy-average calculation and in the following only the results from the six-state calculation will be discussed.

For obtaining more low-lying doublet states the same procedure as that described previously for the quartet states was attempted. An energy-average CASSCF calculation for the two $^2\Delta$ and the two $^2\Sigma^+$ states with separated-atom limits (^{6}D,^{7}S) and (^{6}D,^{5}S) was performed. However, at short internuclear distances the $^2\Delta$ and $^2\Sigma^+$ states highest in energy interfere strongly with one state and two other states, respectively. Instead an energy-average CASSCF calculation for $X^2\Delta$, $A^2\Sigma^+$, $B^2\Delta$, and $C^2\Delta$ was performed for short internuclear distances. The other Σ^+ states are higher in energy. This calculation presented some difficulties. Firstly, for the strongly interfering $B^2\Delta$ and $C^2\Delta$ states a multistate version of CASPT2 [12] had to be used for avoiding crossings. Secondly, the $C^2\Delta$ state correlates with high-lying atomic states at the separated-atom limit, presumably (^{6}D,^{5}G), and therefore it was hard to continue the calculations at intermediate and long bond distances. Thirdly, the energy difference at the CASPT2 level of theory between the $X^2\Delta$ and $A^2\Sigma^+$ states is larger (0.15 eV at equilibrium distances) than in the two-state calculation discussed at the beginning of this section. In the following $X^2\Delta$ and $A^2\Sigma^+$ refer to those resulting from the two-state calculation.

In order to calculate all the lowest-lying electronic states the Π states also have to be considered. The $A^2\Pi$ and $A^4\Pi$ states correlating with the (^{6}D,^{7}S) separated-atom limit were obtained in single-state CASSCF calculations (followed by CASPT2). However, to not break the axial rotational symmetry the point group was reduced to C_2 and the Π states were obtained by making an energy-average CASSCF calculation for the two Π components (Π_x and Π_y) in the actual calculations.

From the procedure described previously hopefully all the lowest-lying states of VCr should be obtained. However, for a complete picture states correlating with the separated- atom limit (^{4}F,^{7}S) should also be studied. An attempt was made to calculate the $A^4\Sigma^-$ state in a single-state calculation. However, owing to large molecular rotations (the CASSCF did not converge) it was only possible to calculate the potential-energy curve for bond distances smaller than 3.75 au, a distance somewhat larger than the optimal bond length for that state.

4 Results and discussion

The results from the calculations discussed in the previous section are summarized in Fig. 1 and Tables

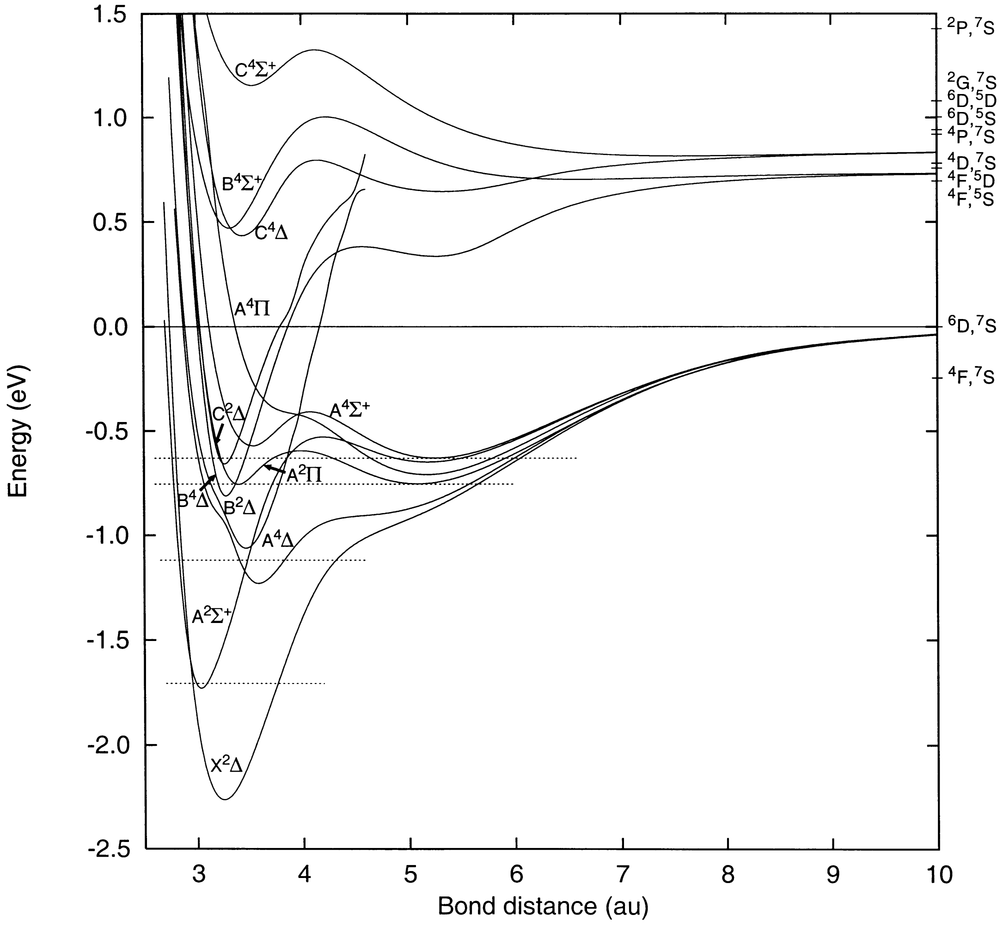

Fig. 1. Potential-energy curves for VCr computed with the complete-active-space self-consistent field/complete-active-space second-order perturbation theory method. The *dotted lines* represent the positions of the measured states relative to the ground state. The levels to the *right* are the experimental separated-atom limits

Table 5. Spectroscopic constants of electronic states of $^{51}V^{52}Cr$. Obtained with the complete-active-space self-consistent-field (*CASSCF*) CAS second-order perturbation theory method using an atomic natural orbital (6s5p4d3f2g) basis set. 3*s* and 3*p* correlation effects are not included. Relativistic corrections are included

State	r_e (Å)	D_e (eV)	ω_e (cm^{-1})	$\Delta G_{1/2}$ (cm^{-1})	T_e (eV)	T_e (cm^{-1})	No.v[a]
$C^4\Sigma^+$	1.870	–	357	334	3.42	27554	3
$B^4\Sigma^+$	1.756	0.276	511	496	2.73	22040	5
$C^4\Delta$	1.819	0.415	446	446	2.70	21747	5
$A^4\Pi$	–	–	–	–	–	–	–
$A^4\Sigma^+$	1.870	0.572	395	377	1.69	13639	3
$A^4\Sigma^-$	1.934	–	564	–	1.61	12962	1
$C^2\Delta$	1.727	–	858	803	1.60	12943	10
$A^2\Pi$	1.796	0.754	503	449	1.51	12150	3
$B^4\Delta$	1.733	1.557	822	776	1.45	11703	10
$B^2\Delta$	1.832	–	607	559	1.20	9687	10
$A^4\Delta$	1.893	1.230	475	445	1.03	8325	5
$A^2\Sigma^+$	1.605	1.730	803	765	0.53	4299	10
$X^2\Delta$	1.720	2.262	568	557	0.00	0	10

[a] The number of vibrational levels used to determine spectroscopic constants

Table 6. Dominant configurations in the CASSCF wavefunction for electronic states of VCr. At the internuclear distance of 3.3 au. To calculate the natural orbitals the keyword SDAV in the restricted-active-space SCF program was set to between 2000 and 4000. The energies of the states were obtained with between two and eight accurate decimals

State	Configuration[a]	Weight
$C^4\Sigma^+$	$(3d\sigma)^2(3d\pi)^4(3d\delta)^3(3d\delta^*)^1(4s\sigma^*)^1$	0.29
	$(3d\sigma)^1(3d\pi)^4(3d\delta)^3(3d\delta^*)^1(4s\sigma)^1(4s\sigma^*)^1$	0.15
	$(3d\pi)^4(3d\delta)^3(3d\delta^*)^1(4s\sigma)^2(4s\sigma^*)^1$	0.06
$B^4\Sigma^+$	$(3d\sigma)^1(3d\pi)^4(3d\delta)^4(4s\sigma)^1(4s\sigma^*)^1$	0.41
	$(3d\sigma)^1(3d\pi)^4(3d\delta)^2(3d\delta^*)^2(4s\sigma)^1(4s\sigma^*)^1$	0.10
$C^4\Delta$	$(3d\sigma)^2(3d\pi)^4(3d\delta)^2(3d\delta^*)^1(4s\sigma)^1(4s\sigma^*)^1$	0.52
	$(3d\sigma)^1(3d\pi)^4(3d\delta)^2(3d\delta^*)^1(4s\sigma)^1(4s\sigma^*)^1$	0.13
$A^4\Pi$	$(3d\sigma)^2(3d\pi)^3(3d\delta)^3(3d\delta^*)^1(4s\sigma)^2$	0.50
$A^4\Sigma^+$	$(3d\sigma)^2(3d\pi)^4(3d\delta)^3(3d\delta^*)^1(4s\sigma)^1$	0.29
	$(3d\sigma)^1(3d\pi)^4(3d\delta)^3(3d\delta^*)^1(4s\sigma)^2$	0.16
	$(3d\sigma)^1(3d\pi)^4(3d\delta)^4(4s\sigma)^1(4s\sigma^*)^1$	0.07
$A^4\Sigma^-$	$(3d\sigma)^2(3d\pi)^4(3d\delta)^2(4s\sigma)^2(4s\sigma^*)^1$	0.71
$C^2\Delta$	$(3d\sigma)^2(3d\pi)^4(3d\delta)^2(3d\delta^*)^1(4s\sigma)^2$	0.32
	$(3d\sigma)^2(3d\pi)^4(3d\delta)^3(4s\sigma)^1(4s\sigma^*)^1$	0.10
	$(3d\sigma)^1(3d\pi)^4(3d\delta)^3(4s\sigma)^2(4s\sigma^*)^1$	0.15
$A^2\Pi$	$(3d\sigma)^2(3d\pi)^3(3d\delta)^4(4s\sigma)^2$	0.51
$B^4\Delta$	$(3d\sigma)^2(3d\pi)^4(3d\delta)^2(3d\delta^*)^1(4s\sigma)^2$	0.37
	$(3d\sigma)^2(3d\pi)^4(3d\delta)^3(4s\sigma)^1(4s\sigma^*)^1$	0.20
$B^2\Delta$	$(3d\sigma)^2(3d\pi)^4(3d\delta)^2(3d\delta^*)^1(4s\sigma)^2$	0.25
	$(3d\sigma)^2(3d\pi)^4(3d\delta)^3(4s\sigma)^1(4s\sigma^*)^1$	0.14
	$(3d\sigma)^1(3d\pi)^4(3d\delta)^3(4s\sigma)^2(4s\sigma^*)^1$	0.17
$A^4\Delta$	$(3d\sigma)^2(3d\pi)^4(3d\delta)^2(3d\delta^*)^1(4s\sigma)^2$	0.24
	$(3d\sigma)^2(3d\pi)^4(3d\delta)^3(4s\sigma)^1(4s\sigma^*)^1$	0.25
	$(3d\sigma)^1(3d\pi)^4(3d\delta)^3(4s\sigma)^2(4s\sigma^*)^1$	0.08
$A^2\Sigma^+$	$(3d\sigma)^1(3d\pi)^4(3d\delta)^4(4s\sigma)^2$	0.49
	$(3d\sigma)^1(3d\pi)^4(3d\delta)^2(3d\delta^*)^2(4s\sigma)^2$	0.11
$X^2\Delta$	$(3d\sigma)^2(3d\pi)^4(3d\delta)^3(4s\sigma)^2$	0.57

[a] For the Δ and Σ^+ states the $3d\sigma$ and $4s\sigma$ natural orbitals are almost equal mixtures of atomic 3*d* and 4*s* orbitals

Table 7. Experimental data of electronic states of $^{51}V^{52}Cr$. From Ref. [4]

ω_e (cm^{-1})	$\Delta G_{1/2}$ (cm^{-1})	T_0 (eV)	No. v[a]
571 ± 8	565 ± 20	1.63	6
758 ± 38	708 ± 20	1.51	4
460 ± 10	440 ± 20	1.14	5
715 ± 11	688 ± 15	0.56	7
520 ± 8	505 ± 10	0.00	10

[a] The number of vibrational levels used to determine spectroscopic constants

5 and 6. The potential-energy curves in Fig. 1 and the corresponding spectroscopic constants (Table 5) are based on results obtained at the CASPT2 level of theory including relativistic corrections (see Sect. 2), while an analysis of the electronic wave functions at the internuclear distance of 3.3 au (summarized in Table 6) is based on results at the CASSCF level of theory. For Fig. 1 it should be mentioned that the energy plotted is the electronic energy difference to the separated-atom limit (^6D,^7S); however, for the $B^2\Delta$ and $C^2\Delta$ states the position of the curves is related to the minimum of the $X^2\Delta$ curve. Further, for the $A^4\Sigma^-$ state the calculated small fragment of the potential-energy curve is not included in Fig. 1; however, it was possible to calculate some spectroscopic constants from it and they have been included in Table 5.

In Fig. 1 the position of the measured states (relative to the ground state) from the work by Alex and Leopold [4, 5] is indicated by dotted lines. The basis of only transition energies (with errors of the order 0.1 eV) possible candidates for the measured states are $A^2\Sigma^+$ for the first state, $A^4\Delta$ and $B^2\Delta$ for the second state, and $B^4\Delta$, $A^2\Pi$, $C^2\Delta$, $A^4\Sigma^-$, and $A^4\Sigma^+$ for the third and fourth states.

Now a more detailed analysis of the measured and calculated states will follow. The experimental data for the five measured states (including the ground state) are collected in Table 7. These data are useful for further identification of the measured states. Starting with the vibrational frequencies the ground state is in error by about 50 cm^{-1}; the first excited state ($A^2\Sigma^+$) is in error by about 90 cm^{-1}. These errors can be expected from the calculations. The vibrational frequencies for the second measured excited state fit with both $A^4\Delta$ and $B^2\Delta$ and are in error by about 5 and 120 cm^{-1}, respectively, for $\Delta G_{1/2}$. From these data it is hard to exclude any of the two states and from Table 6 it is clear that their wave functions are similar. Maybe this measured second excited state consists of two states. With similar arguments the third measured excited state should consist of the two states $B^4\Delta$, and $C^2\Delta$, whose wave functions are similar and whose fundamental vibrational frequencies are in error by about 70 and 100 cm^{-1}, respectively, from the measured value. For the states discussed so far the calculated vibrational frequencies are larger than the measured values. If the same holds for the measured fourth excited state none of the remaining states in Table 5 would do. A presumptive candidate would be the $A^4\Sigma^-$ state, whose calculated vibrational frequency is within the error bars of the experimental value.

The remaining issue to discuss is the bond lengths. The experiments by Alex and Leopold do not provide absolute values of the bond lengths but only values relative to the bond length of the ground state of the VCr anion. However, the calculated bond lengths of the $X^2\Delta$ and $A^2\Sigma^+$ states (1.72 and 1.60 Å) agree well with the values (1.70 and 1.61 Å) obtained in the local density study by Mattar and Doleman [13].

Further support for some of the calculated values is the rotationally resolved spectrum of VCr by Sickafoose et al. [14]. They obtained $r_0 = 1.7260 \pm 0.0011$ Å for the ground state, which fits nicely with the calculated value $r_e = 1.720$ Å for the same state. Further, they identified an excited state at 14371 cm^{-1} (1.78 eV) with $r_0 = 1.7201 \pm 0.0011$ Å. This state fits well with the calculated $C^2\Delta$ state with $r_e = 1.727$ Å and $T_e = 12943$ cm^{-1} (1.60 eV).

5 Conclusions

The electronic spectrum of VCr, altogether 12 states, has been calculated using the CASSCF/CASPT2 approach. The calculated spectrum has been useful in identifying electronic states that appear in the experimental work by Alex and Leopold using negative ion photoelectron spectroscopy [4,5]. However, if the identification is correct there still remain issues that need clarification. For example, from the experimental data of two of the excited states it should be possible to identify two more electronic states with similar energies. The calculations have shown that at the position of the second and third measured excited states there are $^4\Delta$ and $^2\Delta$ states close in energy and with similar wave functions.

The purpose of the present paper has been not only to generate a number of electronic states for aiding the explanation of experimental data, but equally well to present a methodology for calculating potential-energy curves for first-row transition-metal dimers. The CASSCF/CASPT2 method is in this respect successful but as has been illustrated in the present paper the possibility to include more orbitals in the active space is desirable and perhaps would make it possible to describe electronic states correlating with (^{4}F,^{7}S) and (^{6}D,^{7}S) using the same set of orbitals. For example, for the V atom the inclusion of the 4*d* orbitals in the active space reduces the numbers 1.82 and 2.26 eV discussed in the introduction to 0.42 and 0.83 eV, respectively. For molecules, in order to use such large active spaces, a more restricted wave function than the CASSCF, for example the RASSCF, would have to be used. A corresponding RASPT2 program would then have to be constructed.

Acknowledgements. The research reported in this communication was supported by a grant from the Swedish Natural Science Research Council (NFR). S. Alex and D.G. Leopold are acknowledged for providing results from their negative ion photoelectron spectroscopy on VCr.

References

1. Andersson K, Roos BO, Malmqvist PÅ, Widmark PO (1994) Chem Phys Lett 230: 391
2. Andersson K (1995) Chem Phys Lett 237: 212
3. Casey SM, Leopold DG (1993) J Phys Chem 97: 816
4. Alex S (1997) Phd thesis, University of Minnesota, Minneapolis
5. Alex S, Leopold DG (to be published)
6. Andersson K, Malmqvist PÅ, Roos BO, Sadlej AJ, Wolinski K (1990) J Phys Chem 94: 5483
7. Andersson K, Malmqvist PÅ, Roos BO (1992) J Chem Phys 96: 1218
8. Andersson K (1995) Theor Chim Acta 91: 31
9. Roos BO, Andersson K (1995) Chem Phys Lett 245: 215
10. Pou–Amérigo R, Merchán M, Nebot–Gil I, Widmark PO, Roos BO (1995) Theor Chim Acta 92: 149
11. Andersson K, Blomberg MRA, Fülscher MP, Karlström G, Lindh R, Malmqvist PÅ, Neogrady P, Olsen J, Roos BO, Sadlej AJ, Schutz M, Seijo L, Serrano-Andrés L, Siegbahn PEM, Widmark PO (1997) MOLCAS, version 4. Lund University, Sweden
12. Finley J, Malmqvist PÅ, Roos BO, Serrano-Andrés L (1998) Chem Phys Lett 288: 299
13. Mattar SM, Doleman BJ (1994) J Phys Chem 98: 9764
14. Sickafoose SM, Langenberg JD, Morse MD (2000) J Phys Chem A 104: 3521
15. Moore CE (1952) NBS circular 467. US Government Printing Office Washington, DC
16. Herzberg G (1950) Molecular spectra and molecular structure, vol 1. Van Nostrand Reinhold, New York
17. Bondybey VE, English JH (1983) Chem Phys Lett 94: 443
18. Hilpert K, Ruthardt K (1987) Ber Bunsenges Phys Chem 91: 724